PRACE INSTYTUTU ODLEWNICTWA
TRANSACTIONS OF FOUNDRY RESEARCH INSTITUTE

Volume LV Year 2015 Number 3

DOI: 10.7356/iod.2015.14

Solidification path of the AlFeMnSi alloys in a stage of primary intermetallic phases precipitation

Ścieżka krystalizacji w stopach AlFeMnSi podczas powstawania pierwotnych wydzieleń faz międzymetalicznych

Małgorzata Warmuzek[1]

[1] *Instytut Odlewnictwa, Zespół Laboratoriów Badawczych, Laboratorium Badań Struktury i Właściwości, ul. Zakopiańska 73, 30-418 Kraków*

[1] *Foundry Research Institute, Complex of Accredited Research Laboratories, Laboratory for Structure Analysis and Mechanical Testing, 30-418 Kraków, Poland*

E-mail: malgorzata.warmuzek@iod.krakow.pl

Abstract

In this work, an analysis of the solidification course of the AlFeMnSi alloys was carried out in the Al alloys of Fe, Mn, and Si concentrations in a range supplementary for those examined until now. The morphology of the pre-dendrite and pre-eutectic precipitates of the AlFeMnSi intermetallics has been revealed in relation to alloy composition. The phase attribution of the AlFeMnSi intermetallics forming primary pre-dendrite and pre-eutectic crystals was revealed in situ *through local diffraction methods. The results obtained in the present work, as compared with data published previously, revealed the critical limit of the Mn concentration, necessary to stabilize the α_c-AlFeMnSi phase as equal ≤ 0.5 wt.%, in the alloys AlFe≤3.0MnSi6 and AlFe≤1.5MnSi11 and ≥ 0.5 wt. % in AlFe≥3.0MnSi11.*

Key words: Al alloy, AlFeMnSi intermetallics, primary precipitation, solidification path

Streszczenie

W pracy analizowano przebieg procesu krzepnięcia stopów AlFeMnSi podczas powstawania predendrytycznych oraz preeutektycznych faz międzymetalicznych AlFeMnSi w zakresie stężenia składników, uzupełniającym badane dotychczas zakresy. Ujawniono oddziaływanie składu chemicznego stopu na morfologię predendrytycznych oraz preeutektycznych faz międzymetalicznych AlFeMnSi. Charakterystyka wydzieleń faz międzymetalicznych AlFeMnSi została zidentyfikowana in situ*, z zastosowaniem lokalnych metod dyfrakcyjnych. Uzyskane wyniki zostały porównane z danymi opublikowanymi uprzednio. Oszacowano, że krytyczne stężenie manganu, konieczne do stabilizacji fazy α_c-AlFeMnSi, wynosiło ≤ 0,5%, w badanych stopach AlFe≤3,0MnSi6 i AlFe≤1,5MnSi11 oraz ≥ 0,5% w stopach AlFe≥3,0MnSi11.*

Słowa kluczowe: stopy Al, fazy międzymetaliczne, wydzielenia pierwotne, ścieżka krystalizacji

1. Introduction

In the microstructure of the cast AlSi alloys, containing transition metals Fe and Mn, the numerous intermetallic AlFeMnSi phases of different chemical composition (Table 1) and different morphology (Fig. 1) are present. The solidification sequence of alloys, some critical Fe and Mn concentrations were exceeded in, commenced with the AlFeMnSi phases precipitation, prior main microstructure constituents i.e. α-Al dendrites and eutectic (α-Al+Si) appeared [1,2]. Under technological conditions, in the standard AlSi cast alloys, due to non-equilibrium microsegregation of both Fe and Mn, the primary crystallization of the AlFeMnSi intermetallics also occurs, though concentration of these elements is usually lower than critical [1−5]. Primary precipitates are usually considered as undesirable microstructure constituents, because of their gravity segregation in cast parts and the harmful effects on mechanical properties [3−5]. The pre-dendrite or pre-eutectic incongruent solidification $L \rightarrow AlFe(Mn)Si + L_1$ is either bivariant in the ternary AlFeSi [1,6−8] or polyvariant in the quaternary AlFeMnSi alloys [1,9−13]. Liquidus in the Al corner of the Al-Fe-Mn-Si equilibrium diagram in a range of the primary precipitation of AlFeMnSi intermetallics (i.e. Fe ≥ 2 wt.% and

Table 1. Crystal lattice and chemical composition of the intermetallic phases in the AlFeMnSi alloys [1, 7, 9, 11, 13]
Tabela 1. Struktura krystaliczna i skład chemiczny faz międzymetalicznych w stopach AlFeMnSi [1, 7, 9, 11, 13]

Phase/Faza	Crystallographic system / Układ krystalograficzny	Space group / Grupa przestrzenna	Elementary cell / Komórka elementarna			Sublattice model / Model podsieci
			Prototype/ Prototyp	Parameters/ Parametry		
				a nm	c nm	
α_H-AlFeSi	Hexagonal/ Heksagonalny	$P6_3/mmc$	Al_5Co_2	1,238	2,6184	$Al_{0.6612}Fe_{0.19}Si_{0.0496}(AlSi)_{0.0992}$
α_c-AlMnSi	Cubic/Regularny	Pm3	$Al_{102}Mn_{24}Si_{12}$ Al_9Mn_5Si	1,268(2)		$Al_{14}Mn_4Si_1(AlSi)_2$
α_c-AlMnFeSi	Cubic/Regularny	Im3	CsCl	1,265		$Al_{0.598}(FeMn)_{0.152}Si_{0.1}(AlSi)_{0.15}$ $Al_{15}(FeMn)_6Si_1(Al,Si)_4$ $Al_{16}(FeMn)_4Si_1(Al,Si)_2$
β-AlFeSi	Monoclinic/ Jednoskośny	mcm	–	a = 0.612, b = 0.612 c = 4.148, β = 91°		$Al_{0.598}Fe_{0.152}Si_{0.010}(AlSi)_{0.15}$

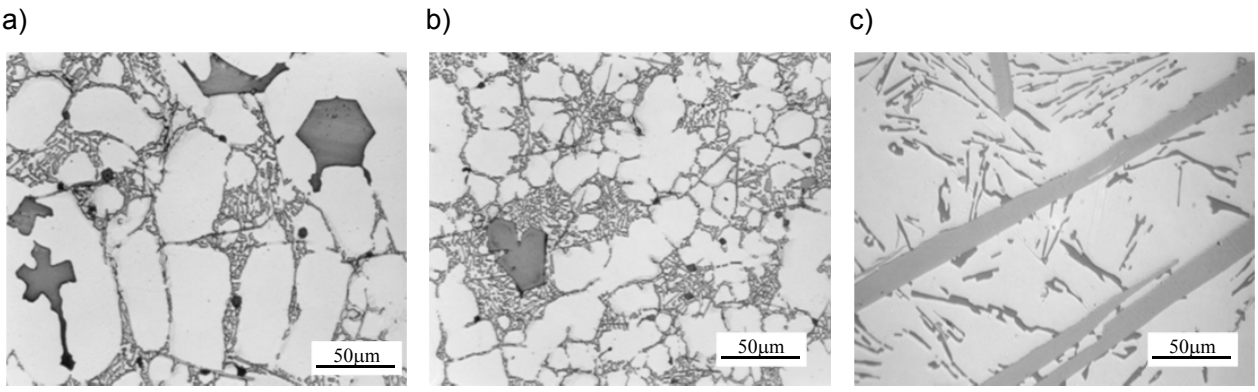

Fig. 1. Primary precipitates of the AlFeMnSi phases, microstructure of the technical AlSi alloys, LM: a) cast part in sand mould, alloy AlSi9Cu, b) cast part in metal mould, alloy AlSi9Cu, c) cast part in sand mould, alloy AlSi11FeMn

Rys. 1. Pierwotne wydzielenia faz AlFeMnSi, mikrostruktura technicznych stopów AlSi, mikroskop świetlny: a) odlew w formie piaskowej, stop AlSi9Cu, b) odlew w formie metalowej, stop AlSi9Cu, c) odlew w formie piaskowej, stop AlSi11FeMn

Si > 3 wt.%),was determined by Phillips [6], Phragmen [7], Zakharov [10], Lacaze [11], Balitchev [12], Abou Khatwa [13]. They are based on either experimental data [6,7,10] or numerical simulation of the solidification path, according to the Scheil model [11−13]. Zakharov [10] identified four AlFeMnSi intermetallics crystallized primarily: quaternary $Al_{16}(FeMn)_4Si_3$ (Fe/Mn = 0.25), and ternaries $Al_{15}Mn_3Si_2$ β-AlFeSi and α_H-AlFeSi. Onderka [15] and Flores [16] estimated the chemical composition of the primary crystals of quaternary AlFeMnSi intermetallic formed in hypo-eutectic alloys as Si9.5 wt.%, Mn0.6−2.20 wt. %, Fe0.8−1.6 wt. % of the variable content of the transition metals (Fe/Mn 1.3−0.7). The different stoichiometry of this AlFeMnSi intermetallic was defined based on its chemical composition: $Al_8MnFeSi_2$ (Fe/Mn = 1) [16], $Al_{0.66}Mn_{0.082}Fe_{0.081}Si_{0.175}$ (Fe/Mn = 0.99) [17], $Al_{11.8}FeMn_{1.6}Si_{1.6}$ (Fe/Mn = 0.63). Although different formulas were ascribed to the revealed quaternary AlFeMnSi phase, the value of the Fe/Mn ratio in each of them was constant as stated in these formulas, regardless of that the Fe/Mn value in that alloy in which the particular AlFeMnSi crystal was precipitated.

Recent studies suggest that the boundary between stability fields of phases α_H-AlFeSi (hexagonal) and α_c-AlFeMnSi (cubic) is situated in a Mn concentration range of < 0.5 wt.%. In the AlSiFeMn0.3 alloys on the liquidus surface, critical Mn concentration was determined by Munson as equal to 0.3 wt.% [14]. Based on the last

result of an analysis of Lacaze's model [12] and results of Davignon studies [17], Raghavan [18] assigned this quaternary α-AlFeMnSi phase to an array of continuous solid solutions AlFeMnSi, based on the structure of the ternary cubic α_c-AlMnSi phase. The upper limit of the Fe concentration in this array was not exactly estimated.

However, as exact stability limits for the three phases β-AlFeSi, α_H-AlFeSi and α_c-AlFeMnSi, forming primary precipitates in the quaternary Al-Fe-Mn-Si system, were not estimated unequivocally until now, alloy microstructure constituents have been formed, which still need *in situ* identification. Especially in the published works, the data concerning hypo-eutectic AlFeMnSi alloys solidification are not present. In this work the microstructure effects in the initial stage of primary precipitates formation was examined in the hypo- and eutectic AlFeMnSi alloys of chemical composition complementary to that in works published previously.

2. Experimental

Materials of examinations have been AlSi alloys, hypoeutectic (Si6 wt.%) and eutectic (Si11.5 wt.%), containing different amounts of the transition metals Fe (1.5 and 3.0 wt.%) and Mn (0.1, 0.5 and 2.0 wt.%).

The sequence of the microstructure constituents formation was analyzed by means of the differential scanning calorimeter using DSC Netsch (at a cooling rate 3−5 K/min). The alloy solidification path was reconstructed on the basis of DSC thermograms and microscopic observations. Alloy microstructure was examined in the specimens frozen from the liquid-solid state at specific temperature, chosen according to the DSC results, by means of the metallographic light microscope Axio-ObserverOZm1 on the polished cross sections (etched with 1% HF reagent) and scanning electron microscope Stereoscan 420 (after deep etching with 10% NaOH reagent). The intermetallic phase precipitates have been identified *in situ* based on their chemical composition, estimated by means of the EDS local microanalysis (Link ISIS300) and on their crystal structure, identified by means of the EBSD analysis (PHILIPS XL30 EBSD EDAX GENESIS – Delphi). Some intermetallic phases were identified by means of the SAED method, using TEM microscope Philips CM20.

3. Results and discussion

Hypoeutectic alloys AlFe1.5Mn0-0.1Si6. In the hypoeutectic alloys two exothermic effects were noticed before the last eutectic reaction L → α-Al+Si + β-AlFeSi started. First exothermic effect at 617°C (AlFe1.5MnSi6) and – at 615°C (AlFe1.5Mn0.1Si6) was related to crystallization of the α-Al solid solution dendrites, typically for all of the AlFeSi alloys, containing Si < 8 wt.% and Fe ~ 1.3 wt.% [9]. The next effects were analyzed by comparison with a solidification course of the AlFe1.5Si5 alloy [9]. After dendrites crystallization, a series of reactions was identified in: monovariant eutectic reaction L → α-Al + α_H-AlFeSi, followed by invariant peritectic reaction L + α_H-AlFeSi → α-Al + β-AlFeSi. This sequence started to develop when liquid composition achieved: 6.5% Si, 1.7% Fe [5,6], then followed by the monovariant eutectic reaction: L → α-Al + β-AlFeSi. Its commencement on the solidification path of the alloys: AlFe1.5Si7 [1] and (AlFe1.3Si6) [7] was reported at 611°C. Based on the observation of the microstructure constituents it might be assumed that the second exothermic effect, at 608°C (AlFe1.5Si6) or 599°C (AlFe1.5Mn0.1Si6), has represented mainly monovariant eutectic reaction: L → α-Al + β-AlFeSi. Precipitates of the β-AlFeSi phase in the form of the long plates were placed in the interdendrite microregions (Fig. 2). However, in the alloy AlFe1.5Mn0.1Si6, the compact particles of the α_H-AlFeSi phase situated near the plates of the β-AlFeSi phase were accidentally visible (Fig. 3).

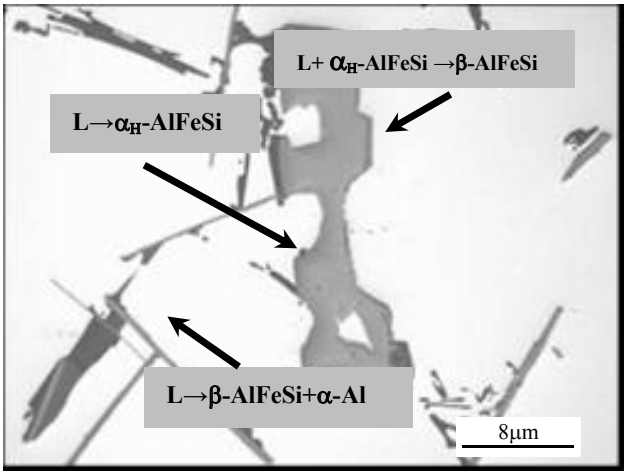

Fig. 3. Microstructure of the hypoeutectic AlFe1.5Mn0.1Si6 alloy, slowly cooled, 3 K/min, LM; polyphase microregion: α-Al + α_H-AlFeSi + β-AlFeSi + Si as a possible product of the peritectic reaction L + α_H-AlFeSi → β-AlFeSi(b)

Rys. 3. Mikrostruktura stopu podeutektycznego AlFe1.5Mn0.1Si6, chłodzonego z prędkością 3 K/min, obszar wielofazowy: α-Al + α_H-AlFeSi + β-AlFeSi + Si, widoczne mikrostrukturalne efekty reakcji perytektycznej: L + α_H-AlFeSi → β-AlFeSi

This microstructure effect might be considered as a product of the peritectic reaction L + α_H-AlFeSi → α-Al + β-AlFeSi, occurring without direct contact of both pro-peritectic and peritectic phases, at 609−607°C. The plate of the β-AlFeSi phase, visible in Figure 3, could then grow at the expense of the components of the α_H-AlFeSi phase simultaneously dissolved. Such a model of the peritectic reaction is recognized in the

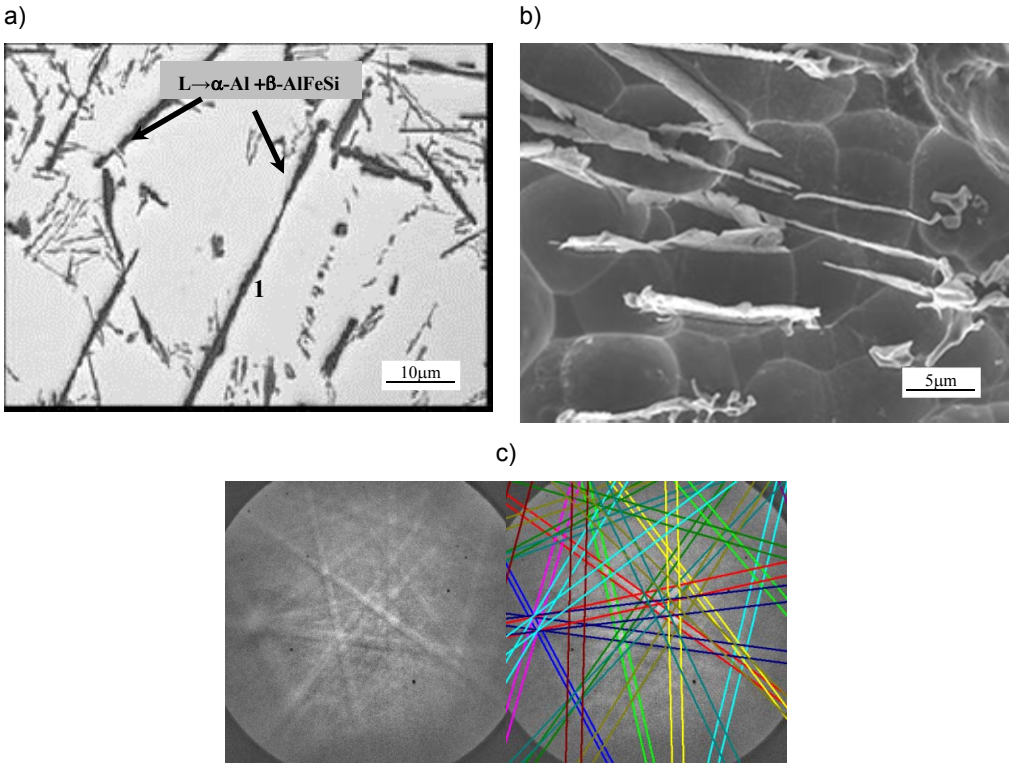

Fig. 2. Microstructure of the alloy hypoeutectic AlFe1.5Si6 alloy, slowly cooled, 3 K/min, pre-dendrtite needles of the β-AlFeSi phase: a) LM, b) SEM and c) EBS diffraction pattern (point 1, Fig. 2a), reference Al9Fe2Si2 phase CI 0.016

Rys. 2. Mikrostruktura podeutektycznego stopu AlFe1.5Si6, chłodzonego z prędkością 3 K/min, predendrytyczne wydzielenia fazy β-AlFeSi w kształcie igieł: a) mikroskop świetlny, b) skaningowy mikroskop elektronowy oraz c) obraz dyfrakcyjny EBS (punkt 1, rys. 2a), faza referencyjna Al9Fe2Si2, CI 0.016

systems with the AlFeMnSi intermetallic phases [19]. Furthermore, the rim of the β-AlFeSi phase (traces), round the pre-peritectic (primary) α_H-AlFeSi phase precipitates in the microstructure of the AlFe1.5Mn0.1Si6 alloy considered as an intermediate stage suggest the possibility of a three-phase peritectic reaction at α-Al/α_H-AlFeSi interface (Fig. 3).

Hypoeutectic alloys AlFe3.0Mn0-0.1Si6. In the microstructure of the AlFe3.0Mn0-0.1Si6 alloys, the AlFeSi particles in a shape of the equiaxed polyhedron were *in situ* identified as α_H-AlFeSi phase (Fig. 4). They were formed through incongruent polyvariant process $L \rightarrow \alpha_H$-AlFeSi + L_1, initiated at either 643°C (AlFe3Si6 alloy) or 645°C (AlFe3Mn0.1Si6 alloy). It means that, in its first stage, solidification of the examined alloys commences according to the solidification path of AlFe2.0Si5 [9] and AlFe2Si6 [7] alloys, extrapolated to higher Fe concentration. The pre-dendrite precipitation of the α_H-AlFeSi phase limit was noticed in a range of concentration: > 2 wt.% Fe and > 3 wt.% Si, according to the liquidus course established by Phillips [6], then proved by Liu [7] and Lacaze [11]. As the field of the primary precipitation of the Al_3Fe phase was shifted to a higher Si content with an increase in the Fe content, some volume fraction of the α_H-AlFeSi phase, observed at room temperature in the AlFe3Si6 alloy, might be a product of the equilibrium invariant peritectic reaction L + $Al_3Fe \rightarrow \alpha_H$-AlFeSi + α-Al (at 629−632°C [6,7]). Nevertheless, neither thermal nor microstructure effects of the primary precipitation of the Al_3Fe phase were revealed.

Two exothermic effects (609°C – AlFe3Si6 alloy, and 607°C – AlFe3Mn0.1Si6 alloy), recorded below primary precipitation of the α_H-AlFeSi phase were assigned to:

1) crystallization of the dendrites of the α-Al solid solution: $L \rightarrow$ α-Al + L_1, initiated at 617°C,

2) invariant peritectic reaction: L + α_H-AlFeSi → α-Al + β-AlFeSi or undercooled monovariant eutectic reactions: L → α-Al + β-AlFeSi (AlFe3Si6) and L → α-Al + α_H-AlFeSi (AlFe3Mn0.1Si6).

The microstructure effects of the peritectic reaction: L + α_H-AlFeSi → α-Al + β-AlFeSi were revealed by Tibballs [20] in AlSiFe3.5Si7.5 and AlFe3Mn0.1Si7.5 alloys after prolonged annealing at high temperature (950°C/12 h + 620°C/30 h). As observed progress of the peritectic reaction in the examined alloys in this work was not advanced significantly, similarly as in Tibballs work [20], volume fraction of the pre-peritectic α_H-AlFeSi phase remained quite large. Thus, the monovariant eu-

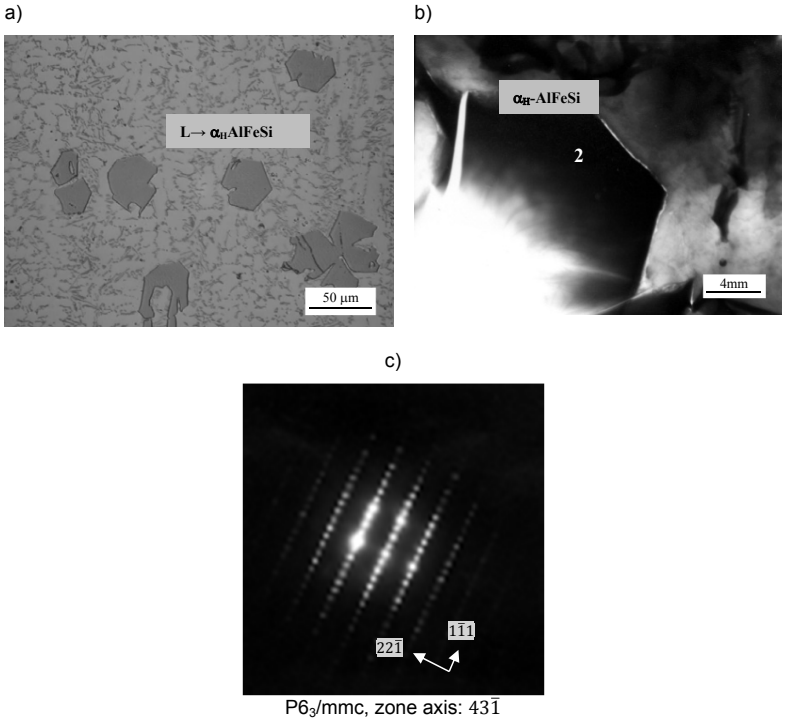

Fig. 4. Microstructure of AlFe3.0Mn0.1Si6 alloy, held at 695°C, then frozen, pre-dendrite equiaxed polyhedron of the α_H-AlFeSi phase: a) LM and b) TEM, c) SAE diffraction pattern (point 2, Fig. 4b)

Rys. 4. Mikrostruktura stopu podeutektycznego AlFe3.0Mn0.1Si6, zamrożona po wygrzewaniu w temperaturze 695°C, predendrytyczne wydzielenie fazy α_H-AlFeSi w postaci równoosiowego wielościanu: a) mikroskop świetlny, b) transmisyjny mikroskop elektronowy oraz c) obraz dyfrakcyjny SAE (punkt 2, rys. 4b)

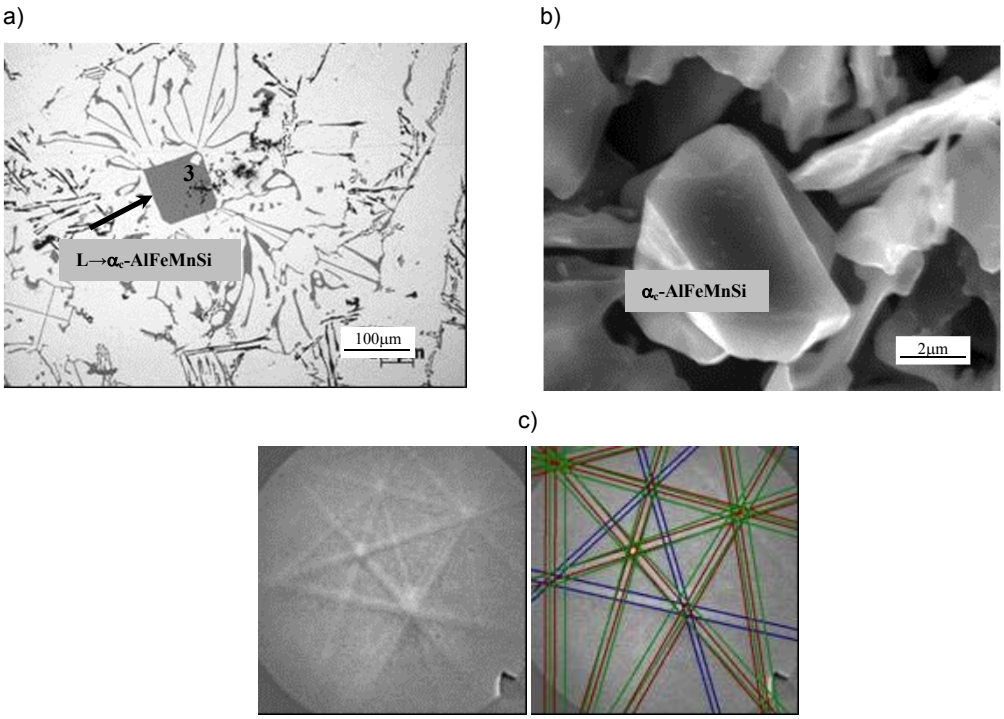

Fig. 5. Microstructure of the AlFe3.0Mn0.5Si6 alloy, cooling rate 3 K/min, pre-eutectic equiaxed polyhedron of the α_c-AlFeMnSi phase: a) LM and b) SEM, c) EBS diffraction pattern (point 3, Fig. 5a), reference cubic phase Al4.01MnSi0.74, CI 0.133

Rys. 5. Mikrostruktura stopu podeutektycznego AlFe3.0Mn0.5Si6, chłodzonego z prędkością 3 K/min, predendrytyczne wydzielenie fazy α_c-AlFeMnSi w postaci równoosiowego wielościanu: a) mikroskop świetlny, b) skaningowy mikroskop elektronowy oraz c) obraz dyfrakcyjny EBS (punkt 3, rys. 5a) faza referencyjna Al4.01MnSi0.74, CI 0.133

tectics effects: α-Al + β-AlFeSi and α-Al + α_H-AlFeSi were recognized as dominating in the microstructure after primary precipitates formed.

Hypoeutectic alloys AlFe1.5-3.0Mn0.5-2.0Si6. Solidification of these alloys started with primary precipitation of the α_c-AlFeMnSi phase (Fig. 5). With an increase in Mn content up to 2.0 wt.%, the temperature of the primary pre-dendrite AlFeMnSi phase formation strongly increased (625°C – AlFe1.5Mn0.5Si6, 699°C – AlFe1.5Mn2.0Si6, 676°C – AlFe3Mn0.5Si6, and 731°C – AlFe3Mn2.0Si6) [2].

According to Tibballs [20], critical Mn content stabilizing cubic structure of the α_c-AlFeMnSi phase in the AlFe3MnSi7.5 alloys was established as ≥ 0.1 wt.% Mn, while, in the AlFe2.5MnSi6 alloys, the lower limit was shifted to a range of 0.2−0.3 wt.% Mn. The results obtained in the present work, as compared with data published previously [10, 12, 13], revealed a critical limit of the Mn concentration, necessary to stabilize the α_c-AlFeMnSi phase in the AlFe1.5-3.0Mn0.5-2.0Si6 alloys equal at least to 0.5 wt.%.

The primary α_c-AlFeMnSi phase solidification has been followed by that of the α-Al solid solution, then, by binary bivariant eutectics, either L → α-Al + α_H-AlFeSi (606°C, Mn 0.5 wt.%) or L → α-Al + α_c-AlFeMnSi (585°C, Mn 2 wt.%). It means that the local composition of the interdendritic liquid was influenced by the pre-dendrite precipitation process. In the AlFe3.0Mn0.5Si6 alloy, in a stage of primary α_c-AlFeMnSi phase crystallization most of the Mn atoms were included in its precipitates, thus, Mn concentration in the interdendritic liquid was insufficient to stabilize the cubic structure of the AlFeMnSi eutectic crystals. Therefore, the Chinese script of the α_H-AlFeSi phase became the main constituent of binary eutectics (Fig. 6).

Eutectic alloys AlFe1.5Mn0-0.1Si11. The individual thermal effects of the incongruent solidification of the β-AlFeSi phase have not been yet recorded separately in the eutectic alloys AlFe1.5Mn0-0.1Si11, although they have been anticipated according to the Al-Fe-Si equilibrium diagram [7, 9, 12, 13].The pre-eutectic thermal effects was assigned as following: that at 580°C in AlFe1.5Si11 alloy to the monovariant eutectic reaction L → Al + β-AlFeSi and that at 591°C in AlFe1.5Mn0.1Si11 alloy to bivariant eutectic reaction: L → Al + β-AlFe(Mn)Si. Since the temperature gap between the end of the anticipated precipitation of the primary β-AlFeSi phase and the start of next process is very narrow (about 10°C), both effects might overlap. Thus, the β-AlFeSi phase precipitates formed through crystallization either incongruent or eutectic (both monovariant and invari-

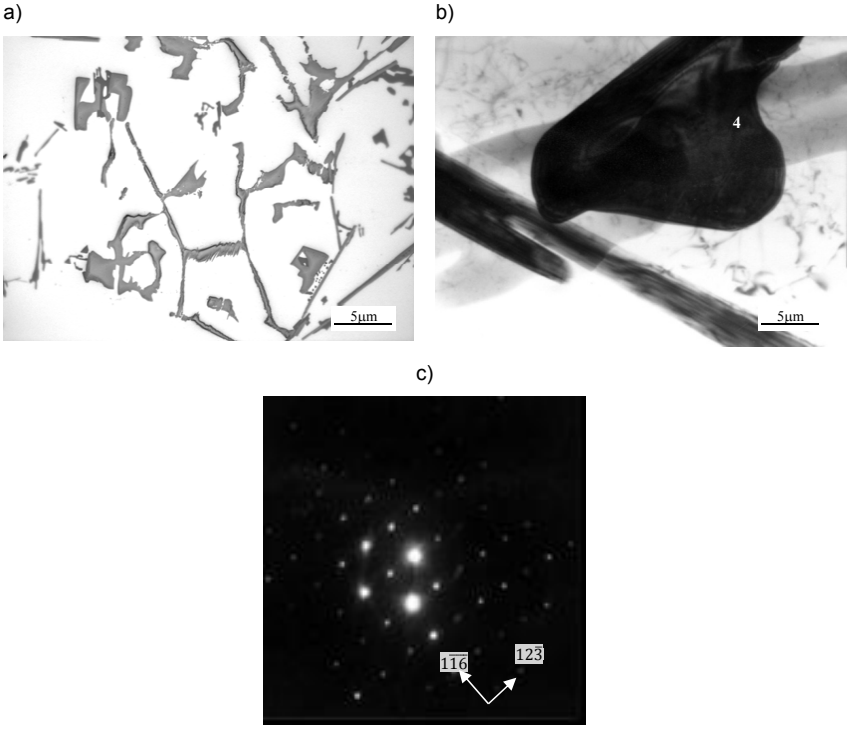

Fig. 6. Microstructure of the AlFe3.0Mn0.5Si alloy, precipitate of the α_H-AlFeSi phase in a shape of the Chinese script, in the eutectic α-Al + α_H-AlFSi: a) LM, b) TEM and c) SAED, diffraction pattern (point 4, Fig. 6b)

Rys. 6. Mikrostruktura stopu podeutektycznego AlFe3,0Mn0,5Si6, wydzielenie fazy α_H-AlFeSi w postaci chińskiego pisma w eutektyce α-Al + α_H-AlFSi: a) mikroskop świetlny, b) transmisyjny mikroskop elektronowy oraz c) obraz dyfrakcyjny SAED (punkt 4, rys. 6b)

ant), though they have been difficult to distinguish, even in the frozen microstructure.

Eutectic alloys AlFe3.0Mn0-0.1Si11. Solidification commenced with primary precipitation of the β-AlFeSi phase in the shape of elongated plates (Fig. 7). This process was previously revealed experimentally in AlFe3Si10 alloys [10], and then confirmed by numerical simulation of the Scheil model in alloys AlFe1-3Si10 and AlFe1-3Si14 [12,13]. Temperature of the primary precipitation of the β-AlFeSi phase is almost stable in a wide range of the Si content (10−14 wt.%), while it is strongly influenced by Fe content [7,10,12]. It increases from 605°C (1 wt.% Fe) to 670°C (3 wt.% Fe) [10]. According to Liu [7], primary precipitation of the β-AlFeSi phase takes place in a temperature range from 670°C (2 wt.% Fe) to 620°C (5 wt.% Fe). In the present work, the commencement of primary precipitation of the β-AlFeSi phase was noticed in the AlFe3Si11 alloy at 637°C and in the AlFe3Mn0.1Si11 alloy – at 641°C, thus, good interpolation of data was obtained with alloys AlFeSi10, containing either 2 or 5 wt.% Fe.

In the examined area of the Al-Fe-Mn-Si equilibrium diagram, incongruent precipitation of the primary β-AlFeSi phase (Al-Fe2-Si isopleths [9]) was followed by the sequence of two eutectic reactions: monovariant and invariant. The monovariant eutectic L → Al + β-AlFeSi commenced according to [9,13] at 590°C, while in the examined alloys it was revealed at 583°C. Then, it developed in a temperature range overlapping that of the solidification of the invariant eutectic L → Al + Si + β-AlFeSi.

Eutectic alloys AlFe1.5-3.0Mn0.5-2.0Si11. The primary precipitates of the AlFeMnSi phases crystallized in a typical shape of the polyhedra more or less equiaxed, visible in the microstructure in Figures 8 and 9. In the AlFe1.5.Mn0.5-2.0.Si11 alloys, precipitation of the α_c-AlFeMnSi phase crystals was identified in the form of the equiaxed polyhedra at 617°C and 673°C, respectively. This result is consistent with that obtained previously by Zakharov [10] and Balitchev [12] in the AlFe1MnSi10 alloys, as it constitutes an interpolation of their data to higher concentrations of both Fe and Si. In the AlFe3.0Mn0.5Si11 alloy the primary precipitates were identified as α_H-AlFe(Mn)Si phase (Fig. 8). Therefore, this attribution was not consistent with the results published previously by Zakharov [10] and Balitchev [11] for the AlFe3MnSi10 alloys, as they reported primary precipitation of the β-AlFeSi phase, before the Mn concentration reached 0.8 wt.% [13]. Abou Khatwa and Malakhov [13] reported primary precipitation of the β-AlFeSi phase at 669°C until Mn concentration in the alloy reached 1 wt.%. Furthermore, in the alloy

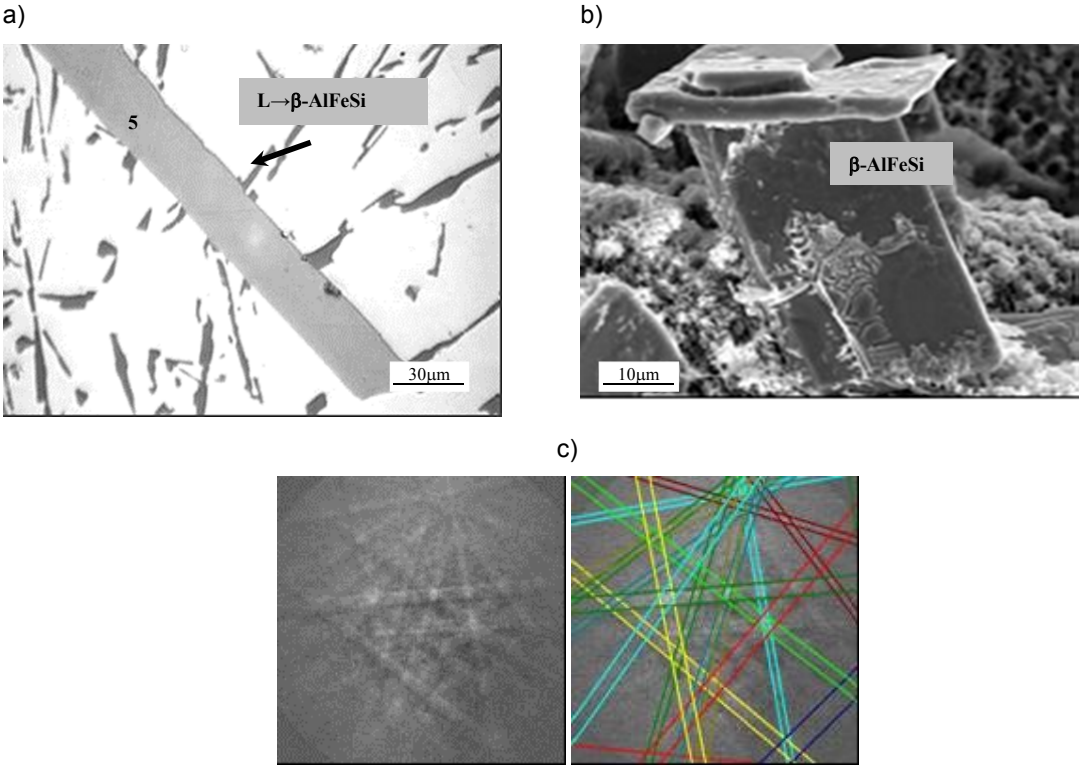

Fig. 7. Microstructure of AlFe3.0Mn0.1Si11 alloy, cooling rate 3 K/min, pre-eutectic plate polyhedron of the β-AlFeSi phase: a) LM and b) SEM, c) EBS diffraction pattern (point 5, Fig. 7a), reference monoclinic phase Al9Fe2Si2, CI 0.341

Rys. 7. Mikrostruktura stopu eutektycznego AlFe3,0Mn0,1Si11, chłodzonego z prędkością 3 K/min, pre-eutektyczne wydzielenie fazy β-AlFeSi: a) mikroskop świetlny, b) skaningowy mikroskop elektronowy oraz c) obraz dyfrakcyjny EBS (punkt 5, rys. 7a) faza referencyjna Al9Fe2Si2, CI 0,341

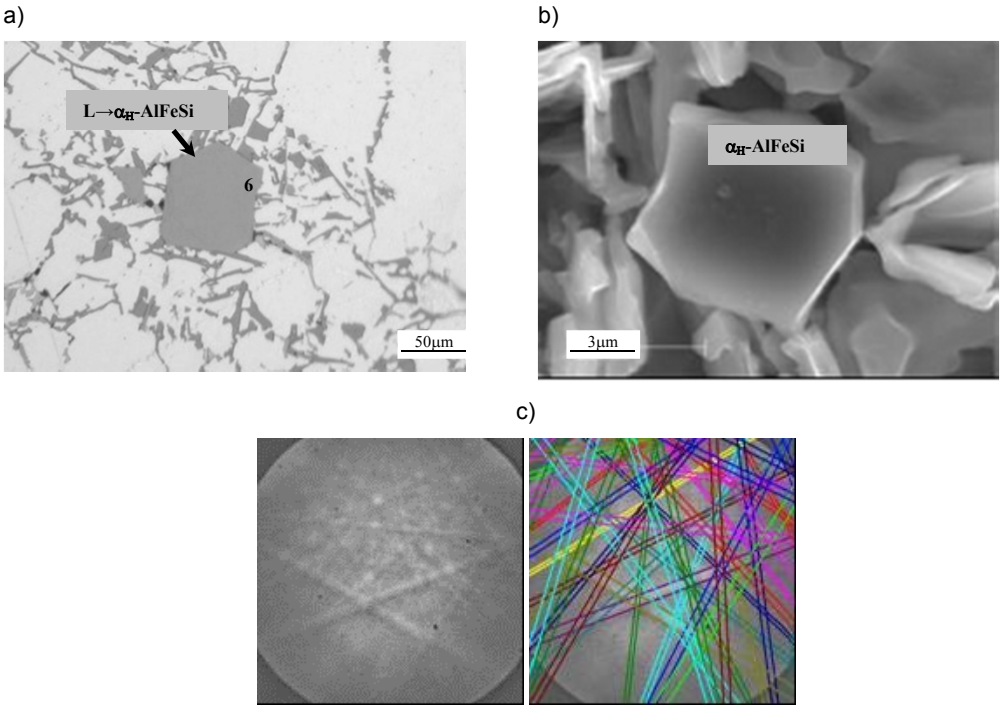

Fig. 8. Microstructure of the AlFe3.0Mn0.5Si11 alloy, cooling rate 3 K/min, pre-eutectic particle of the α_H-AlFeSi phase: a) LM, b) SEM and c) EBS diffraction pattern (point 6, Fig. 8a), reference hexagonal phase: Al8Fe2Si, CI 0.52

Rys. 8. Mikrostruktura stopu eutektycznego AlFe3,0Mn0,5Si11, chłodzonego z prędkością 3 K/min, preeutektyczne wydzielenie fazy α_H-AlFeSi: a) mikroskop świetlny, b) skaningowy mikroskop elektronowy, c) obraz dyfrakcyjny EBS (punkt 6, rys. 8a) faza referencyjna Al8Fe2Si, CI 0,52

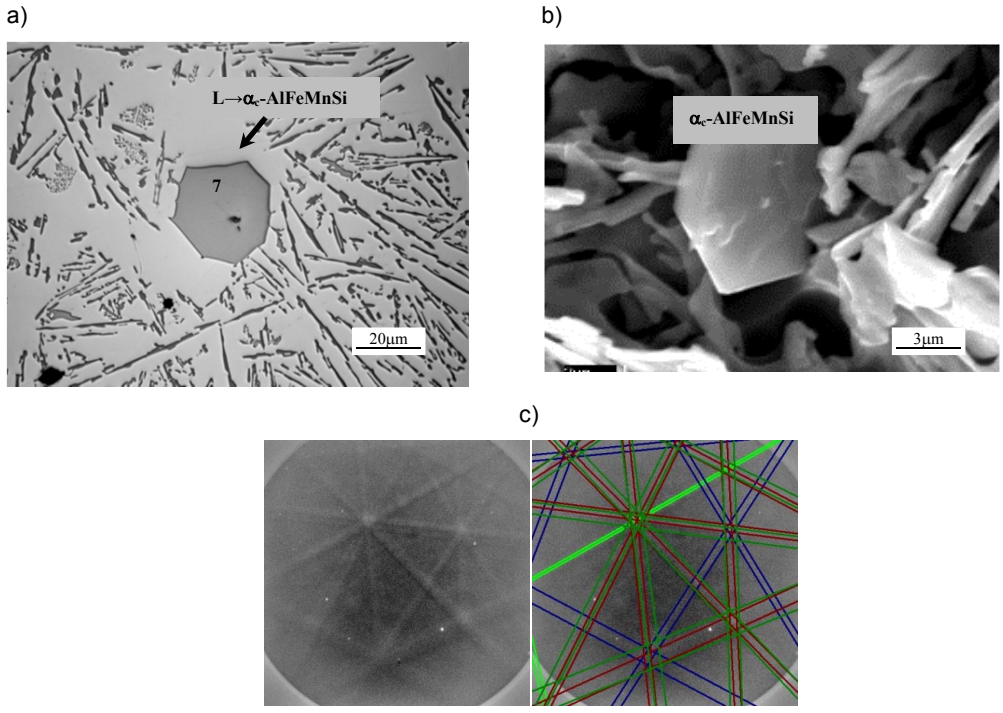

Fig. 9. Microstructure of the AlFe3.0Mn2.0Si11 alloy, cooling rate 3 K/min; pre-eutectic equiaxed polyhedron of the α_c-AlFeMnSi phase: a) LM and b) SEM, c) EBS diffraction pattern, reference cubic phase Al4.01MnSi0.74 CI 0.108 (point 7, Fig. 9a)

Rys. 9. Mikrostruktura stopu eutektycznego AlFe3,0Mn0,5Si11, chłodzonego z prędkością 3 K/min, preeutektyczny wielościan fazy α_c-AlFeMnSi: a) mikroskop świetlny, b) skaningowy mikroskop elektronowy, c) obraz dyfrakcyjny EBS (punkt 7, rys. 9a) faza referencyjna Al4,01MnSi0,74 CI 0,108

AlFe2MnSi10, Lacaze [12] revealed the lower limit of Mn for the primary field of the α_H-AlFe(Mn)Si phase as equal to about 0.25 wt.%.

Only one thermal effect, at 706°C, assigned to pre-eutectic precipitation was recorded in the eutectic alloy AlFe3.0Mn2.0Si11. The quaternary AlFeMnSi phase was ascribed to the equiaxed polyhedra (Fig. 9). This is consistent with the results of Zakharov [10], Balitchev [12], Abou Khatwa [13] and Lacaze [11].

As the quaternary phase was *in situ* identified as cubic phase, isomorphic to α_c-AlMnSi, the results obtained in this work confirmed those published by Davignon [17], Donnadieu [21] and Kim [22]. They revealed a continuous array of the AlFeMnSi solid solutions based on the crystal lattice of the cubic α_c-AlMnSi phase in a wide range of contents of the transition metals Fe and Mn. All of the primary precipitates of this cubic quaternary phase, analyzed in this work, have contained transition metals, both Fe and Mn with Fe/Mn ratio directly related to that in the examined alloy [2].

4. Summary conclusions

1. In the initial stage of the crystallization of the AlFeMnSi alloys, the primary precipitation of the intermetallic phase crystals in the shape of plates, equiaxed polyhedra, and Chinese script was revealed. The crystals were attributed to β-AlFeSi (alloys AlFe1.5Mn0-0.1Si6, AlFe1.5Mn0-0.1Si11 AlFe3Mn0-0.1Si11), α_H-AlFeSi (alloys AlFe3Mn0-0.1Si6, AlFe3Mn0.5Si11) and α_c-AlFeMnSi (AlFe1.5-3Mn0.5-2.0Si6, AlFe3Mn2.0Si11).

2. The results obtained in the present work, as compared with data published previously, revealed the critical limit of the Mn concentration, necessary to stabilize the α_c-AlFeMnSi phase as equal ≤ 0.5 wt.%, in the alloys AlFe≤3.0MnSi6 and AlFe≤1.5MnSi11 and ≥ 0.5 wt.% in those AlFe≥3.0MnSi11.

3. In the AlFe3.0Mn0.5-2.0Si6 alloys, primary–pre-dendrite precipitation of the α_c-AlFeMnSi phase has been followed by α-Al solid solution solidification, then, by binary bivariant eutectics either L → α-Al + α_H-AlFeSi (606°C, wt. 0.5% Mn) or L → α-Al + α_c-AlFeMnSi (585°C, wt. 2% Mn). This means that the local composition of the interdendrite liquid was influenced by pre-dendrite precipitation. As in the stage of primary α_c-AlFeMnSi phase crystallization Mn atoms were included in their precipitates, residual Mn concentration in the interdendrite liquid was insufficient to stabilize the cubic structure of its eutectic crystals.

4. The concentration limit of Mn of primary precipitation of the β-AlFeSi phase in the eutectic alloys (AlFe1.5-3.0MnSi11) was estimated as equal ≥ 0.5 wt.% Mn, which is a value lower than that reported previously in the literature [10, 11, 13].

Acknowledgment

This work was realized with financial support of Polish Ministry of Science and Higher Education under grant No. NN507 378735. Author wish to thank PhD. Sonia Boczkal from OML of Non-Ferrous Metals Institute in Skawina for co-operation in the EBSD examinations, Prof. Jerzy Morgiel from Institute of Materials Engineering and Metallurgy of PAS in Kraków for co-operation in SAEDP analysis and PhD. Andrzej Gazda from Foundry Research Institute in Kraków for carrying out DSC analysis.

References

1. Mondolfo, L. (1976). *Aluminum alloys: structure and properties*. Boston – London: Butter Worths.
2. Warmuzek, M., Ratuszek, W., Sęk-Sas, G. (2005). Chemical inhomogeneity of intermetallic phases precipitates formed during solidification of the Al-Si alloys. *Mater. Charact.*, *54*(1), 31−40.
3. Shabestari, S.G. (2004). The effect of iron and manganese on the formation of intermetallic compounds in aluminum-silicon alloys. *Mat. Sci. Eng. A*, *383A*(2), 289−298.
4. Pucella, G., Samuel, A.M., Doty, H.W., Valtierra, S. (1998). Sludge formation in Sr-modified Al-11.5wt%Si die casting alloys. *AFS Trans.*, 107, 117−125.
5. Shabestari, S.G., Gruzleski J.E. (1994). The effect of solidification condition and chemistry on the formation and morphology of complex intermetallic compounds in aluminum-silicon alloys. *Cast Metals*, *6*(4), 217−224.
6. Phillips, H.W.L. (1946). The constitution of alloys of aluminum with magnesium, silicon and iron. *J. Institute of Metals*, *72*, 151−242.
7. Liu, Z.-K., Chang Y.A. (1999). Thermodynamic assessment of the Al-Fe-Si system. *Met. Mat Trans. A*, *30A*, 1081−1095.
8. Phragmen, G. (1950). On the phases occurring in alloys of aluminum with copper, magnesium, manganese, iron, and silicon. *J. Institute of Metals*, *77,* 489−552.
9. Belov, N.A., Eskin, D.G., Askenov, A.A. (2005). *Multi-component phase diagrams. Applications for commercial aluminum alloys*. Amsterdam: Elsevier.
10. Zakharov, A.M., Gulcyn, I.T., Arnold, A.A., Macenko, J.A. (1988). Fazovyje ravnovesia v systemie Al-Si-Fe-Mn v intervale koncentracji 10−14% Si, 0−3% Fe i 0−4% Mn. *Izv. VUZ, Cvetn. Met.*, (4), 89−94.
11. Lacaze, J., Eleno, L., Sundman, B. (2010). Thermodynamic assessment of the aluminum corner of the Al-Fe-Mn-Si system. *Met. Mat. Trans. A*, *41A*, 2208−2215.

12. Balitchev, E., Jantzen, T., Hurtado, I., Neuschütz, D. (2003). Thermodynamic assessment of the quaternary system Al-Fe-Mn-Si in the Al-rich corner. *Computer Coupling of Phase Diagrams and Thermochemistry*, *27*(3), 275−278.
13. Abou Khatwa, M.K., Malakhov, D.V. (2006). On the thermodynamic stability of intermetallic phases in the AA6111 aluminum alloy. *Computer Coupling of Phase Diagrams and Thermochemistry*, *30*, 159−170.
14. Munson, D. (1967). A clarification of the phases occurring in aluminum–rich aluminum–iron-silicon alloys, with particular reference the ternary phase α-AlFeSi. *J. Institute of Metals*, *95*, 217−219.
15. Onderka, B., Sukiennik, M., Fitzner, K. (2000). Determination of the stability of AlFeMn Si phase existing in the quaternary Al-Fe-Mn-Si system. *Arch. Metall.*, *45*(3), 119−132.
16. Flores-Valdes, A., Sukiennik, M., Castillejos-E., A.H., Acosta-G.,F.A., Escobedo-B., J.C. (1998). A kinetic study on the nucleation and growth of the $Al_8FeMnSi_2$ intermetallic compound for aluminum scrap purification. *Intermetallics*, *6*(3), 217−227.
17. Davignon, G., Serneels, A., Verlinden, B., Dealaney, L. (1996). An isothermal section at 550°C in the Al-rich corner of the Al-Fe-Mn-Si system. *Metall. Mat. Trans. A*, *27A*, 3357−3361.
18. Raghavan, V. (2007). Al-Fe-Mn-Si. *J. Phase Equilib. Diffusion*, *28*, 215−217.
19. Warmuzek, M. (2011). Microstructure evolution during peritectic process L + Al_6Mn(Fe) → α-Al + α(AlMnFe) Si in the AlFeMnSi alloys. *Prace Instytutu Odlewnictwa*, *51*(1), 35−57.
20. Tibballs, J.E., Horst, L.A., Simensen, C.J. (2002). Precipitation of α-Al(Fe,Mn)Si from the melt. *J. Mater. Sci.*, *36*, 937−941.
21. Donnadieu, P., Lapasset, G., Sandersc, T.H. (1994). Manganese-induced ordering in the α-(AlMn-Fe-Si) approximant phase. *Phil. Mag. Let.*, *70*(5), 319−326.
22. Kim, H.Y., Park, T.Y., Han, S.W., Lee, H.M. (2006). Effects of Mn on the crystal structure of α-Al(Mn,Fe) Si particles in A356 alloys. *J. Cryst. Growth*, *291*(1), 207−211.